NUMERICAL SIMULATION OF A SEMITRAILER'S LATERAL PROTECTION SYSTEM AGAINST CAR FRONTAL CRASH

David Valladares Hernando
Dpto. de Ingeniería Mecánica – Universidad de Zaragoza
Grupo VEHIVIAL "Nuevas Tecnologías en Vehículos y Seguridad Vial"
David Fernández Lacruz
Dpto. de Ingeniería Mecánica – Universidad de Zaragoza
Luis Castejón Herrer
Dpto. de Ingeniería Mecánica – Universidad de Zaragoza
Grupo VEHIVIAL "Nuevas Tecnologías en Vehículos y Seguridad Vial"
Hugo Malón Litago
Dpto. de Ingeniería Mecánica – Universidad de Zaragoza
Grupo VEHIVIAL "Nuevas Tecnologías en Vehículos y Seguridad Vial"
Pablo Luque
Ingeniería e Infraestructura de los Transportes – Universidad de Oviedo
Daniel Álvarez Mántaras
Ingeniería e Infraestructura de los Transportes – Universidad de Oviedo

ABSTRACT

The present study is focused on the dynamic simulation of a car frontal crash against a lateral protection system for semitrailers. This system is a barrier fixed laterally to each side in semitrailers, designed to reduce damages on car passengers in case of lateral collision. From the basis of an already existing design, different designs and finite element models where created, adapting the system to the European regulation UNECE nº 73, concerning lateral protection devices' homologation. Finite element models were developed and different materials were considered on the metallic barrier beams. Then, crash simulations using the software LS-DYNA were performed, where a passenger car Toyota Yaris Sedan (2010 model) was impacted against the barrier at 50 km/h, 90 km/h and 120 km/h. Results such as maximum car displacements and deceleration on passengers could be analysed in these simulations. It was assessed the possibility of achieving a weight reduction of the barrier by means of design and material modifications.

1. INTRODUCTION

Current European lateral protection devices installed in semitrailers are designed according to UNECE regulation no 73 (UNECE, 2011), which is focused on the protection of vulnerable road users such as pedestrians, cyclist and motorcyclist, preventing them from being dragged and ran over by the semitrailer's wheels in the event of a collision. In this sense, this regulation defines dimensional, strength and stiffness requirements for the lateral protection systems. Nevertheless, this regulation does not offer protection for more aggressive impacts such as those in which a car collides head-on against the lateral of the semitrailer. In many of these accidents, the car passes through the semitrailer and its roof is torn apart, often resulting in fatal consequences for the car occupants. Considering all kind of vehicles, it can be pointed out that fatalities in lateral and frontal-lateral collisions represented 12% of the total casualties (at 24 h) reached between 2015-2019 at Spanish intercity roads (Observatorio Nacional de Seguridad Vial, 2021). It is also reported that considering all kind of accidents involving heavy goods vehicles in the European Union during 2016-2018, the share of car occupants killed in collisions accounted for 50% of all deaths (Adminaité-Fodor & Jost, 2020). Therefore, it seems plausible that future safety developments and regulations contemplate this type of collision and include more stringent stiffness and strength requirements for lateral protection devices, in the same way as current rear protection systems assembled to semitrailers are demanded to protect car occupants in frontal collisions. In this sense, in the U.S. a new regulation on mandatory requirements to prevent side and front underride accidents was discussed in the “Stop Underrides Act” (H.R.1511, 2019). Crash simulation with finite element software offers the possibility of modeling and simulating the crash behavior of new protection devices at lower costs than actual tests where vehicles are needed to be crashed; in order to guarantee an accurate numerical-experimental correlation several prototypes should always be tested, though. For instance, simulations performed with LS-DYNA could greatly contribute to estimate the vehicles’ crash performance, when new designs of lateral protection systems are included in the model. In order to explore simulation possibilities on this scenario, this paper is focused on the finite element simulation of a semitrailer’s lateral protection system in a car frontal crash situation, with the car colliding perpendicularly to the semitrailer. It was analyzed not only the device’s mechanical performance for different materials and geometric configurations, but also the deceleration reached inside the car and the car displacement when is running at different speed values before hitting.

2. MATERIALS AND METHODS

2.1 “AngelWing” side guard

On the one hand, the starting point was an already existing lateral protection system called “AngelWing” developed by the manufacturer “Airflow deflection” (airflowdeflector, 2021). It was assembled to both sides of a semitrailer and then crash-tested by the IIHS (Insurance Institute for Highway Safety) in 2017 against a Chevrolet Malibu (2009 model) impacting frontally. The test proved that the passive safety offered by this truck side guard prevents the car from underrunning the semitrailer: according to the manufacturer, the guard prevents Passenger Compartment Intrusion at speeds of up to 64.37 km/h (40 mph). Therefore, this device added to other car safety devices such as seat belts, airbags, proximity sensors and emergency brake systems, can highly improve the survival chances for the car occupants. This guard was made of galvanized ASTM A500 steel beams, its global dimensions were

6090×584×2565 mm and its weight was 364 kg; according to the manufacturer, this guard is currently sold by length and truck application.

2.2 Regulation no 73

On the other hand, European regulation no 73 contains the requirements that lateral protection devices (LPD) for vehicles of categories N2, N3, O3 and O4 must comply for their approval in the European Community. Concerning the analysis included in this paper, it has been considered a semitrailer with a maximum mass exceeding 10 tonnes, which corresponds to vehicle category O4 (European Parliament, 2007). The following points, extracted from regulation no 73, detail the dimensional requirements established for LPD in O4 vehicle category:

- LPD shall not increase the overall width of the vehicle and the main part of their outer surface shall not be more than 150 mm inboard from outermost plane of the vehicle. Their rearward end shall not be more than 30 mm inboard from the outermost edge of the rear tyres over at least the rearmost 250 mm.
- LPD may consist of a continuous flat surface, or of one or more horizontal rails, or a combination of surface and rails: when rails are used they shall be not more than 300 mm apart and not less than 100 mm high and essentially flat (O4 case).
- The forward edge of LPD shall be not more than 250 mm to the rear of the transverse median plane of the support legs, if support legs are fitted, but in any case the distance from the front edge to the transverse plane passing through the centre of the kingpin in its rearmost position may exceed 2.7 m.
- Where the forward edge lies in an open space of more than 25 mm, the edge shall consist of a continuous vertical member extending over the whole height of the device; the outer and forward faces of this member shall measure at least 100 mm rearwards and be turned 100 mm inwards or have a minimum radius of 100 mm.
- The rearward edge of LPD shall not be more than 300 mm forward of the vertical plane perpendicular to the longitudinal plane of the vehicle and tangential to the outer surface of the tyre on the wheel immediately to the rear; a continuous vertical member is not required on the rear edge.
- The lower edge of LPD shall at no point be more than 550 mm above the ground.
- The upper edge of LPD shall not be more than 350 mm below that part of the structure, cut of contacted by a vertical plane tangential to the outer surface of the tyres.

With respect to strength and stiffness performance, regulation nº 73 defines the following requirements:

- LPD shall be essentially rigid, securely mounted (not liable to loosening due to vibration) and made of metal or any other suitable material. LPD shall be considered suitable if they are capable of withstanding a horizontal force of 1 KN applied perpendicularly to any part of their external surface by the centre of a ram the face of which is circular and flat, with a diameter of 220 mm ± 10 mm, and if the deflection of the device under load measured at the centre of the ram is then not more than 30 mm over the rearmost 250 mm of the device; and 150 mm over the remainder of the device.

As stated before, while these mechanical requirements are focused on protecting vulnerable road users, it is clear that they are not stringent enough to avoid severe damages in high energy collisions such that with a car hitting the device laterally. For instance, rear protection systems are required to reach much higher forces when tested according to regulation no 58 (UNECE, 2017), with a maximum of 100 KN or 180 KN depending on the location of the points tested.

2.3 Finite element models created for the lateral protection systems

Taking into account all the previous considerations, three different finite element (FE) models were created. Figure 1 shows the six-post model and its main structural dimensions. It used shell elements and consisted of four longitudinal beams (100×100×3 mm) joined by six vertical posts (100×50×3 mm) at each side and six sets of crossed beams (100×50×3 mm) transversally connected to the posts. Bolted and weld joints were simplified by means of equivalent nodes between adjacent parts. Two more variants were created as a simplification from this model: three-post model and two-post model, which are showed in figure 2 and were also analysed.

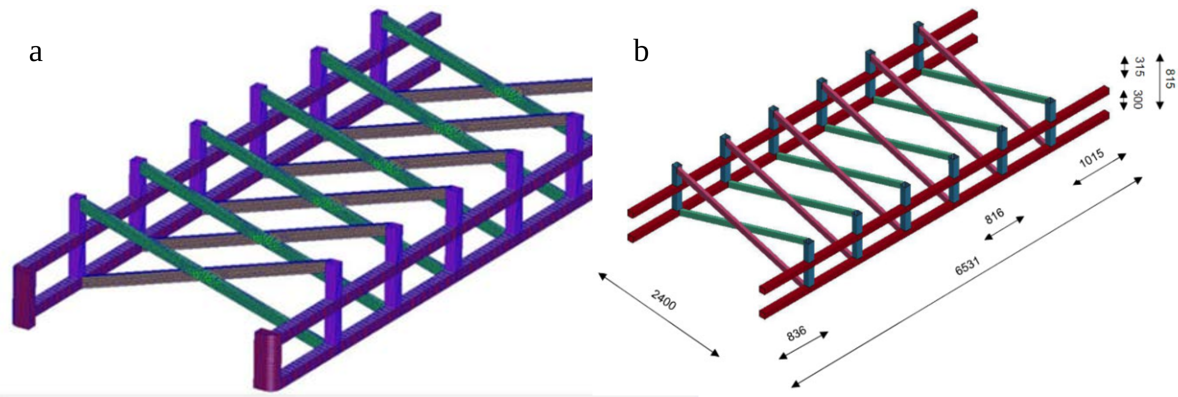

Figure 1: (a) Six-post lateral protection system's FE model; (b) Main structural dimensions

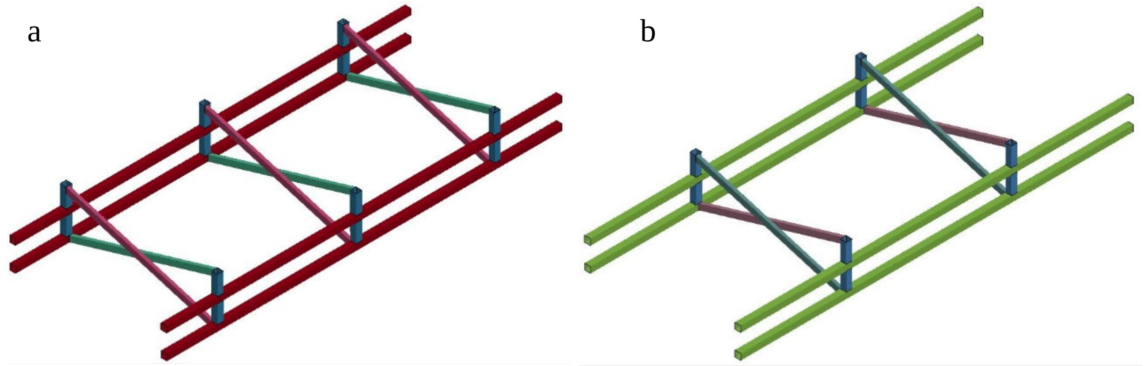

Figure 2: (a) Three-post lateral protection system's FE model; (b) Two-post lateral protection system's FE model

All were modeled using 4-node shell elements with Hughes-Liu formulation and a mesh size of 20 mm. They were created with the software MSC Patran and later on imported in LS-DYNA prepost. The crash behavior of each model was simulated and compared using three different materials for the whole system: S275 (structural steel), Strenx Tube 700MH (high strength steel) and AL 6005A T6 (aluminium alloy with cooling in press). Table 1 shows the main mechanical properties of materials considered in the models and table 2 shows the total weight that resulted from each lateral protection system design.

Material		Density (kg/m^3)	Young modulus (MPa)	Poisson ratio	Yield strength (MPa)	Ultimate strength (MPa)	Elongation at break (°/₁)
Steel	S275 [8]	7850	210000	0.33	275	500	0.2
	Strenx Tube 700MH [9]	7850	210000	0.33	700	850	0.1
Aluminium	6005A – T6 [10]	2710	69500	0.33	215	255	0.08

Table 1: Mechanical properties of materials considered in the FE models

Material		Six-post model Weight (kg)	Three-post model Weight (kg)	Two-post model Weight (kg)
Steel	S275	526.61	388.58	342.60
	Strenx Tube 700MH			
Aluminium	6005A – T6	184.77	137.12	121.25

Table 2: Total weights of the lateral protection systems simulated

2.4 Finite element car model for the crash simulation

All the crash simulations were performed using LS-DYNA, and the FE car model was a Toyota Yaris Sedan (2010), which is available at the National Highway Traffic Safety Administration (NHTSA) web page and has been used in support of several NHTSA programs (NHTSA, 2021). This FE car model was developed by a reverse engineering process at the George Washington University National Crash Analysis Center (NCAC). Its collision performance has been validated with the NCAP 5677 and 6221 tests against a rigid wall (impacting at 40.23 and 56.32 km/h) and it presents also a robust response for the study of a variety of crash scenarios (Marzougui et al., 2012; NCAC, 2011). This model consists of 1480422 nodes and 1514068 elements and it is showed in Figure 3.

3. CALCULATION. BOUNDARY CONDITIONS AND LOAD CASES

In the first place, the EuroNCAP (European new car assessment programme) full width frontal impact test against a concrete barrier (Euro NCAP, 2019) was used as reference, in order to assess the car's deceleration values obtained during the collision against the lateral protection system. The concrete barrier was simulated with rigid shell elements, as showed in figure 3. In this case the car was simulated impacting at 50 km/h, 90 km/h and 120 km/h speed. Since the total mass of the car was 1306.29 kg, the kinetic energies involved in the collision were respectively 125994.49 J, 408215.62 J and 711274.9 J. It can be noted that, starting at a collision speed of 50 km/h, an increase of 40 km/h leads to 3.2 times higher kinetic energy and an increase of 70 km/h leads to 5.6 times higher kinetic energy. Being the wall completely rigid, these simulations represent a highly unfavorable crash situation where all the plastic strain energy was absorbed by the car structure (mainly by the front structural components).

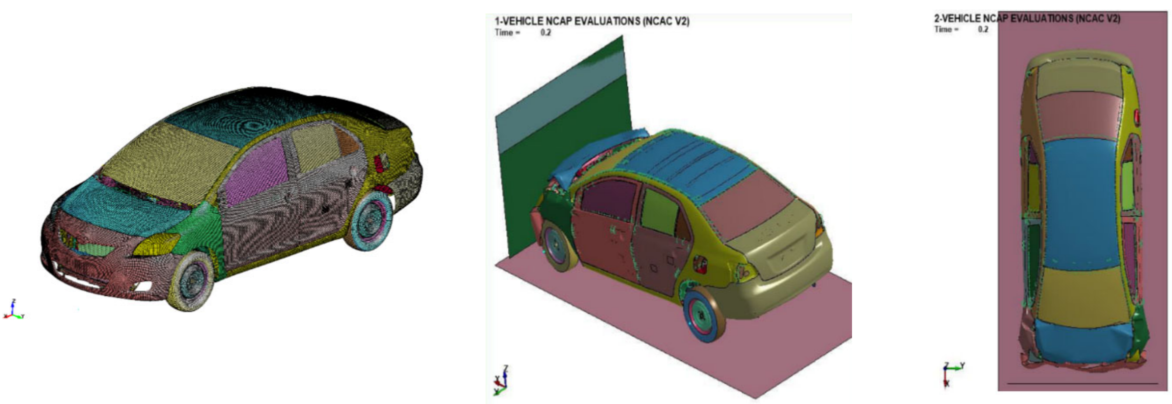

Figure 3: NCAC's FE model for the 2010 Toyota Yaris Passenger Sedan and EuroNCAP full width frontal impact test simulation

In this way, the deceleration results obtained for the lateral protection systems simulated later on, could be compared with these previous results obtained colliding the car frontally against a rigid wall. A rigid shell element simulated the ground and all the nodes of both the wall and the ground were fully constrained (all linear and rotational degrees of freedom). An initial velocity condition was applied to all nodes of the vehicle, with an additional rotational velocity at those nodes comprising the wheels' parts; it also included the gravity acceleration and a general contact condition applied to all the elements of the model.

Regarding the crash simulations for the lateral protection systems analysed, an equivalent approach was considered. In this case, all the nodes located at the top of the vertical posts were fully constrained, corresponding to those regions welded or bolted to the semitrailer's structure. This boundary condition represented a much stiffer situation than what occurs in reality, since the semitrailer's structure could also absorb some strain energy during the collision. Moreover, depending on the energy level involved, among other factors, the semitrailer could even gain kinetic energy and be pushed laterally by the car through the ground. Therefore, the simulations performed were conservative and peak deceleration values reached inside the car were expected to be higher under simulation conditions than under real conditions.

Figure 4 shows the constrained nodes at the top of the posts beams (blue posts in the figure) and the numerical model for simulating the collision against the six-post lateral protection system. In all simulations performed for this study, the car was positioned colliding at the centre of the barrier.

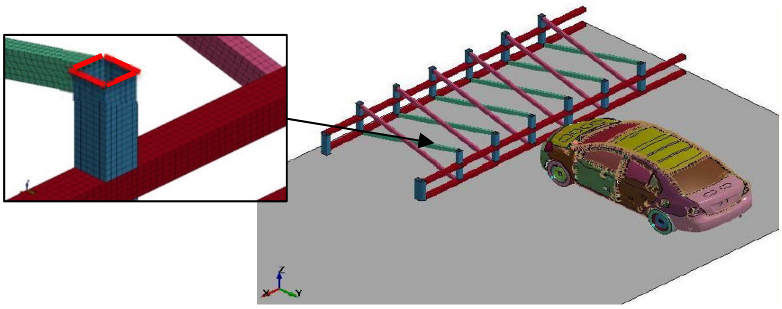

Figure 4: Numerical model simulating a collision against the six-post lateral protection system. Detail with constrained nodes at the top of the posts

4. RESULTS AND DISCUSSION

4.1 Variation in the lateral protection system's geometry

Once the models were created, the first analysis was focused on comparing the performance of the three different designs considered. Figure 5 shows the final frame at the end of each simulation, all calculated with the car impacting at 50 km/h and applying S275 steel to the barriers. While the six-post and the three-post systems were able to stop the car and performed correctly, the two-post system was not stiff enough and collapsed completely. The car model has an accelerometer positioned at its center of gravity for registering the acceleration inside the vehicle. Since the impact time is around 0.14 s, the impact's frequency is near 7 Hz. Then, a 7-Hz low-pass SAE filter was applied to the acceleration signal in order to filter higher frequencies. The car deceleration values, measured in g's, and the car total displacements registered during these simulations can be seen in figures 6 and 7 respectively.

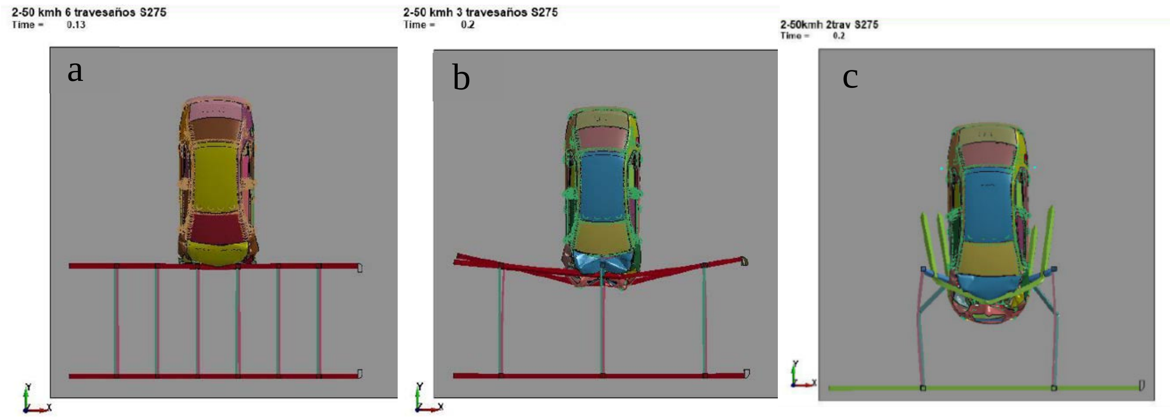

Figure 5: Final frame for simulations at 50 km/h with S275 lateral protection systems: (a) Six-post system; (b) Tree-post system; (c) Two-post system

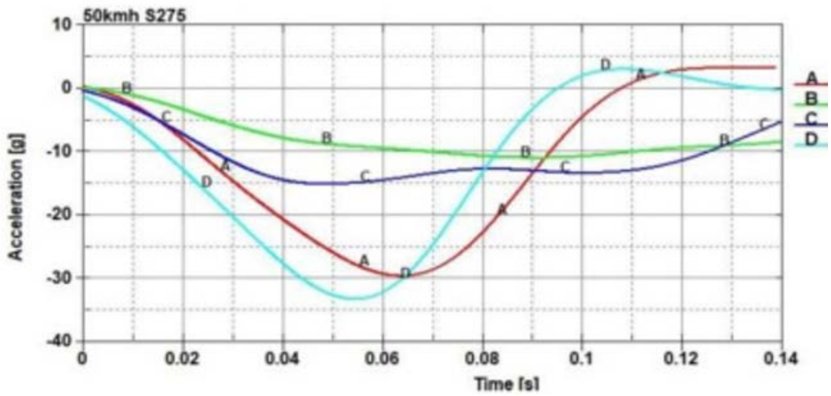

Figure 6: Car deceleration (g's) for simulations at 50 km/h with S275 lateral protection systems: (A) Six-post system; (B) Two-post system; (C) Three-post system; (D) NCAP rigid wall

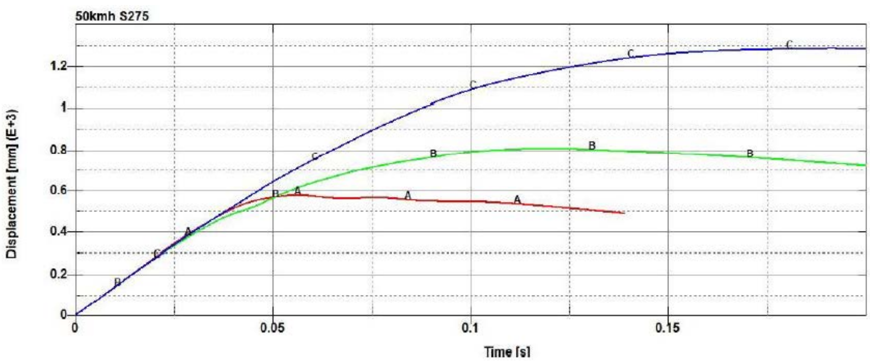

Figure 7: Car displacements (mm) for simulations at 50 km/h with S275 lateral protection systems: (A) Six-post system; (B) Three-post system; (C) Two-post system

While the two-post system collapsed and was not able to stop the car properly, with a displacement value of 1.2 m, the other two systems stopped the car with quite lower displacement values: 0.8 m in the two-post system and near 0.57 m in the six-post system. From these graphs, it can be observed that the three-post system produced a maximum deceleration of 15 g’s and the six-post system produced a maximum deceleration of 30 g’s. Therefore, the three-post design was preferred to the six-post design. The latter performed with a much stiffer response, with its peak deceleration very close to the rigid wall’s one (approximately 33 g’s).

4.2 Variation in the lateral protection system’s material

In order to compare the performance for the three materials considered (steel S275, high strength steel Strenx 700 MH and aluminium alloy 6005 A-T6), the three designs were simulated applying the same material to all barrier components, at each case. Figure 8 shows the final frame at the end of each simulation for the six-post system. Likewise, they were all calculated with the car impacting at 50 km/h.

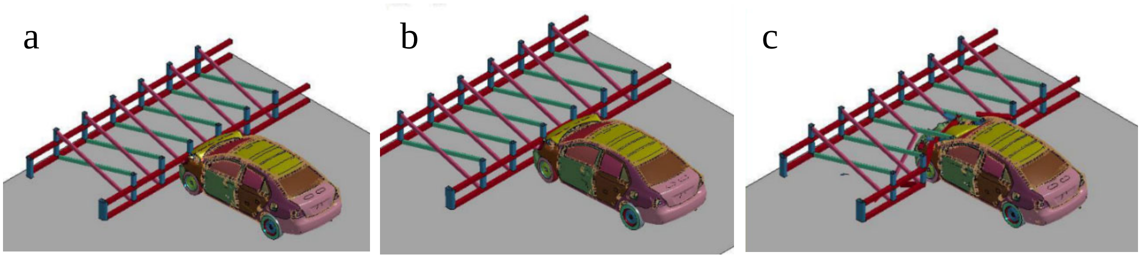

Figure 8: Final frame for simulations at 50 km/h with different materials in the lateral protection systems: (a) S275; (b) Strenx 700 MC; (c) AL 6005A-T6

Figure 9 shows the deceleration values for the simulations with the six-post design, as well as the NCAP rigid wall test’ deceleration values (in g’s). Figure 10 shows the car displacement values in mm.

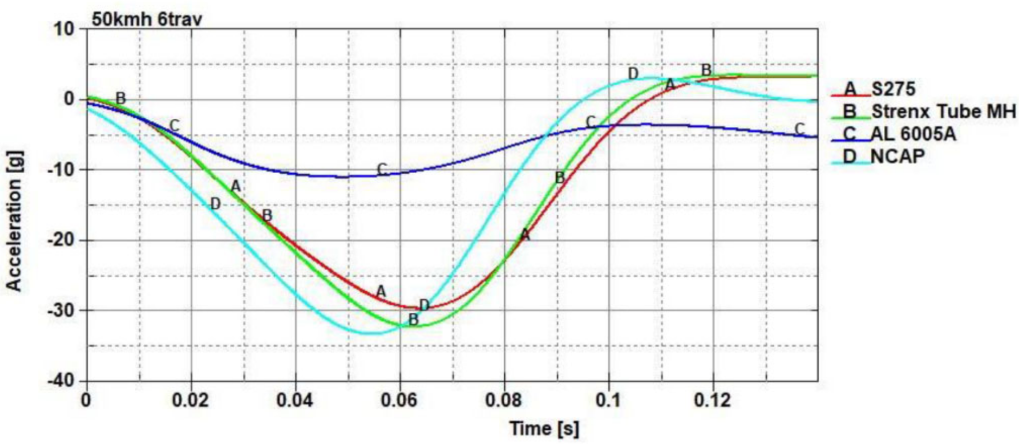

Figure 9: Car deceleration (g’s) for simulations at 50 km/h applying different materials to the six-post system: (A) S275; (B) Strenx 700 MH; (C) AL 6005A-T6; (D) NCAP rigid wall

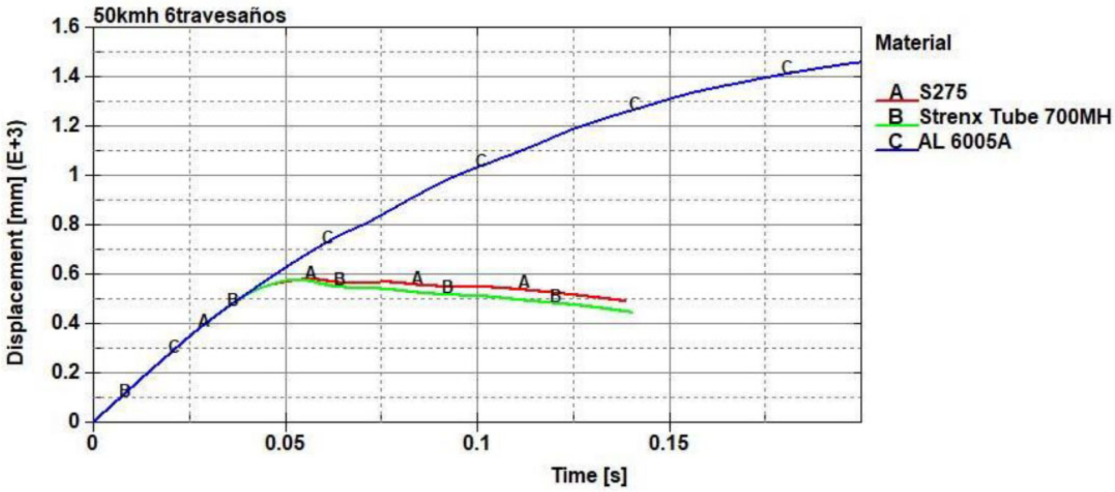

Figure 10: Car displacement (mm) for simulations at 50 km/h with different materials in the lateral protection systems: (A) S275; (B) Strenx 700 MH; (C) AL 6005A-T6

As can be observed from figure 9, the application of high strength steel gave a closer response to the rigid wall collision simulation. However, the aluminium design could not stop the vehicle, with the barrier failing and the car passing through it, as can be observed from figure 10. Both steel systems showed a maximum car displacement of approximately 0.57 m.

4.3. Variation in car's impact velocity

The performance of the lateral protection system with the car colliding at different speed values was also assessed. A collision case at 50 km/h could correspond to an urban road, but, depending on the road category and the speed limits allowed, the lateral collision may take place with the car running at higher speeds.

In order to analyze the system's response at higher kinetic energies, all designs were also simulated applying initial velocities of 90 km/h and 120 km/h. Figure 11 shows the final frame of the simulations with the car impacting at 50 km/h, 90 km/h and 120 km/h, all against the same three-post S275 design.

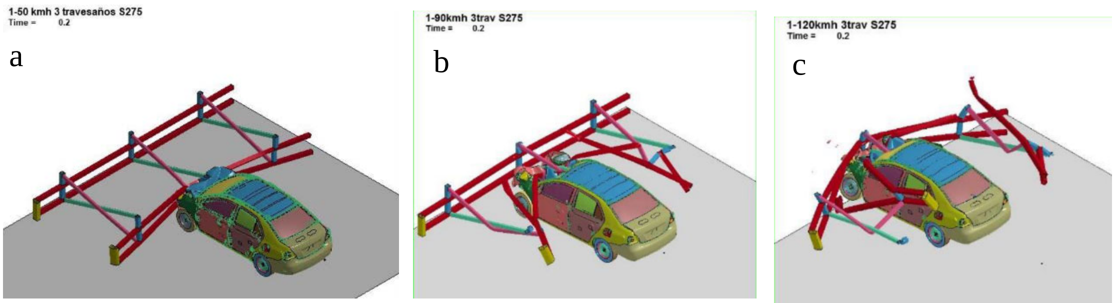

Figure 11: Crash against S275 three-post system: (a) 50 km/h; (b) 90 km/h; (c) 120 km/h

As can be observed in figure 11 (a), the S275 three-post protection system was able to stop the car impacting at 50 km/h, with the energy absorption shared between the protection system and the car's frontal.

Nevertheless, at higher collision speeds of 90 km/h and 120 km/h, the device could not stop the car due to the higher energies involved (respectively, 3.2 and 5.6 times as much as the 50 km/h case), which led the barrier to a full collapse. In both cases the car would continue its movement through the semitrailer, which would be fatal for the car occupants. Figure 12 shows the car deceleration values measured in g's for these simulations. Figure 13 shows the car displacement values in mm.

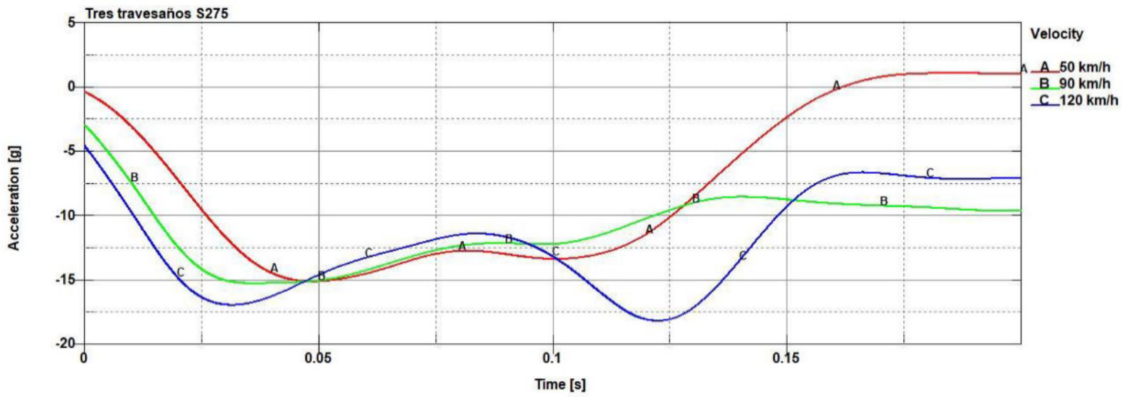

Figure 12: Car deceleration (g's) for S275 three-post system: (A) 50 km/h; (B) 90 km/h; (C) 120 km/h

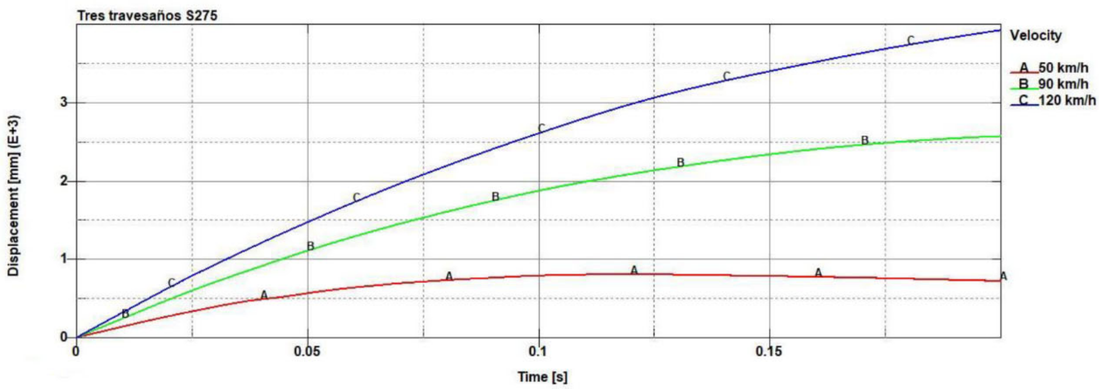

Figure 13: Car displacement (mm) for S275 three-post system: (A) 50 km/h; (B) 90 km/h; (C) 120 km/h

5. CONCLUSIONS

Crash simulation numerical tools can contribute to develop efficient and effective lateral protection systems for semitrailers. On the one hand, in order to improve safety in frontal-lateral car-semitrailer collisions, these systems should be able to resist a certain kinetic energy level as well as to avoid the underrun phenomenon. On the other hand, taking into account that semitrailers must normally cover long range travels, it is desirable to produce light designs that do not lead to an increase in fuel consumption and CO_2 emissions. It has been analysed a car frontal crash against a lateral protection system for semitrailers adapted to the European regulation by means of finite element dynamic simulations performed with the software LS-DYNA. Three different models were created using beam with rectangular hollow sections, referred to as the two-post, three-post and six-post lateral protection systems, varying their number of posts and cross-members. Three different materials were compared: S275 structural steel, Strenx Tube 700MH high strength steel and aluminium alloy 6005A T6. Lastly, three different car impact speeds where simulated: 50 km/h, 90 km/h and 120 km/h.

For simulations with the car running at 50 km/h, the aluminium stiffest design (the six-post one) was not able to resist the energy level involved. Therefore, all aluminium alloy designs were discarded despite their lower weights. At 50 km/h, the two-post system performed poorly in general, all producing underrun situations. On the contrary, the six-post system was found to be excessively stiff in both structural steel and high strength steel models, producing high deceleration peak values inside the car, that could damage the occupants. Then, at that speed, the intermediate three-post system with S275 was the preferred option in terms of cost, weight and safety. The car stopped with a 15 g's peak deceleration and the strain energy was absorbed with better balance by both the barrier and the car.

Therefore, this design could be supposed to perform adequately in urban roads. However, when the car was launched at 90 km/h and 120 km/h, the three-post system was not able to stop the car, and the underrun would be fatal to its occupants. As the kinetic energy level in these collisions depends on the mass and the speed of the car, the results suggest that these lateral protection systems could be designed to offer a proper response at a certain kinetic energy range. A trade-off between peak deceleration values and the allowable car displacement due to the barrier deformation will always be necessary. For instance, although highly stiff designs could lead to peak decelerations near to the rigid wall test's values and would probably add a higher structural weight, they could possibly avoid the car underrun in non-urban road accidents.

REFERENCES

ADMINAITÉ-FODOR, D., JOST, G. (2020). European Transport Safety Council. How to improve the safety of goods vehicles in the EU? May 2020.

AIRFLOWDEFLECTOR (2021). https://airflowdeflector.com/ (accessed 26/02/2021).

EURO NCAP (2019)., Full Width Frontal Impact Testing Protocol, Version 1.2, June 2019, European New Car Assessment Programme.

EUROPEAN PARLIAMENT (2007). Directive 2007/46/EC of the European Parliament and of the Council of 5 September 2007 establishing a framework for the approval of motor vehicles and their trailers, and of systems, components and separate technical units intended for such vehicles.

H.R.1511 (2019). https://www.congress.gov/bill/116th-congress/house-bill/1511 (accessed 26/02/2021)

MARZOUGUI D., SAMAHA R.R., CUI C., KAN C.-D., (2012), Extended Validation of the Finite Element Model for the 2010 Toyota Yaris Passenger Sedan. Workin paper NCAC 2012-W-005, July 2012

NCAC (2011). Development and Validation of a Finite Element Model for a 2010 Toyota Yaris Sedan, NCAC 2011-T-001, prepared for FHWA, December 2011.

NHTSA (2021). https://www.nhtsa.gov/crash-simulation-vehicle-models (accessed 18/03/2021)

OBSERVATORIO NACIONAL DE SEGURIDAD VIAL (2020). Dirección General de Tráfico. Ministerio del Interior. Siniestralidad mortal a 24h en 2020, VÍAS INTERURBANAS. Datos provisionales. Enero 2021.

SABATER FUNDIMOL. http://www.sabater-fundimol.com/es/http://www.sabater-fundimol.com/es/ (accessed 18/03/2021)

SSAB. https://www.ssab.com/ (accessed 18/03/2021)

UNECE (2011). Uniform provisions concerning the approval of: I. Vehicles with regard to their lateral protection devices (LPD). II. Lateral protection devices (LPD). III. Vehicles with regard to the installation of LPD of an approved type according to part II of this regulation. E/ECE/324/Rev.1/Add.72/Rev.1-E/ECE/TRANS/505/Rev.1/Add.72/Rev.1.

UNECE (2017). Regulation No. 58. Uniform provisions concerning the approval of: I. Rear underrun protective devices (RUPDs). II. Vehicles with regard to the installation of an RUPD of an approved type. III. Vehicles with regard to their rear underrun protection (RUP). E/ECE/324/Rev.1/Add.57/Rev.3 – E/ECE/TRANS/505/Rev.1/Add.57/Rev.3. November 2017.

UNE-EN 10025-2:2020. Hot rolled products of structural steels - Part 2: Technical delivery conditions for non-alloy structural steels. AENOR